Water-processable, biodegradable and coatable aquaplastic from engineered biofilms

Anna M. Duraj-Thatte [1,2,3,9], Avinash Manjula-Basavanna [2,3,9],
Noémie-Manuelle Dorval Courchesne [2,4,9], Giorgia I. Cannici [2,5], Antoni Sánchez-Ferrer [6],
Benjamin P. Frank[7], Leonie van't Hag [6], Sarah K. Cotts[8], D. Howard Fairbrother[7], Raffaele Mezzenga [6]
and Neel S. Joshi [1,2,3] ✉

Petrochemical-based plastics have not only contaminated all parts of the globe, but are also causing potentially irreversible damage to our ecosystem because of their non-biodegradability. As bioplastics are limited in number, there is an urgent need to design and develop more biodegradable alternatives to mitigate the plastic menace. In this regard, we report aquaplastic, a new class of microbial biofilm-based biodegradable bioplastic that is water-processable, robust, templatable and coatable. Here, *Escherichia coli* was genetically engineered to produce protein-based hydrogels, which are cast and dried under ambient conditions to produce aquaplastic, which can withstand strong acid/base and organic solvents. In addition, aquaplastic can be healed and welded to form three-dimensional architectures using water. The combination of straightforward microbial fabrication, water processability and biodegradability makes aquaplastic a unique material worthy of further exploration for packaging and coating applications.

Living cells have a remarkable capability to make complex molecules, materials and minerals from abundantly available benign components under ambient conditions. With advances in biomanufacturing and synthetic biology, living cells are being engineered to manufacture a wide range of chemicals, drugs and fuels[1]. This microbially based biomanufacturing strategy extends into polymers, which are an attractive way to make biodegradable bioplastics. In the past few years, the concept of living factories has extended to include not just molecular biosynthesis, but also biologically directed materials fabrication, leading to the emergence of a new field entitled engineered living materials (ELMs)[2–4]. So far, ELMs that can bind to synthetic surfaces, catalyze reactions, sequester chemicals and be used for many other applications have been demonstrated[5–12]. In this Article, we present a report of microbial biofilms engineered to produce a new class of bioplastic, which we have termed aquaplastic, as an alternate composition and approach to biodegradable bioplastics fabrication.

Plastic pollution is a worsening environmental problem that stems from the inherent non-degradability of most conventional plastics, leading to their accumulation in landfills, oceans and waterways[13]. Several approaches have been proposed to address this global challenge, including the development of next-generation recycling technologies and biodegradable bioplastics. A niche approach involves the use of water-soluble or water-dispersible plastics in applications where water resistance is not a main requirement, for example in primary packaging. Polyvinyl alcohol (PVA) is the most prevalent water-soluble plastic used in a wide range of applications related to packaging and coatings[14]. Although bulk materials composed of PVA can dissolve in water, the polymer is

synthesized from petrochemically derived ethylene by free-radical polymerization. Moreover, PVA has consistently been found to have limited biodegradation (several months to years) in natural-solid matrices such as soil and compost, as well as in water bodies that lack PVA-degrading microbes[14]. Plastics that can be produced from biological components in water offer greener fabrication methodologies than those obtained from synthetic and non-biodegradable components in non-aqueous media. Moreover, microbially derived biodegradable bioplastics are attractive alternates to conventional plastics as they offer a more holistically sustainable life cycle.

Here, we demonstrate aquaplastic as a new water-processable bioplastic that is fabricated directly from bacterial culture with minimal purification and can be processed easily from a hydrogel state to form bulk materials (Fig. 1a–c). The mechanical properties of aquaplastic are comparable to petrochemical plastics and other bioplastics. Additionally, aquaplastic possesses unique water-processable characteristics that we term aqua-molding, aqua-welding and aqua-healing.

Results

Fabrication of aquaplastic. Aquaplastic is composed of recombinantly produced biofilm matrix proteins. Biofilms are communities of microbial cells embedded in an extracellular matrix that provides them with adhesion capabilities and protection from the surrounding environment[15]. We leverage the curli system of *Escherichia coli*, which is the primary proteinaceous component of its biofilm matrix, formed by the secretion and extracellular self-assembly of CsgA protein monomers into a fibrous mesh[16]. In previous work, we have demonstrated that a refactored curli expression system can

[1]John A. Paulson School of Engineering and Applied Sciences, Harvard University, Cambridge, MA, USA. [2]Wyss Institute for Biologically Inspired Engineering, Harvard University, Boston, MA, USA. [3]Department of Chemistry and Chemical Biology, Northeastern University, Boston, MA, USA. [4]Department of Chemical Engineering, McGill University, Montreal, Quebec, Canada. [5]Department of Biomedical Engineering, Tufts University, Medford, MA, USA. [6]Department of Health Sciences and Technology, ETH Zürich, Zurich, Switzerland. [7]Department of Chemistry, Johns Hopkins University, Baltimore, MD, USA. [8]TA Instruments, New Castle, DE, USA. [9]These authors contributed equally: Anna M. Duraj-Thatte, Avinash Manjula-Basavanna, Noémie-Manuelle Dorval Courchesne. ✉e-mail: ne.joshi@northeastern.edu
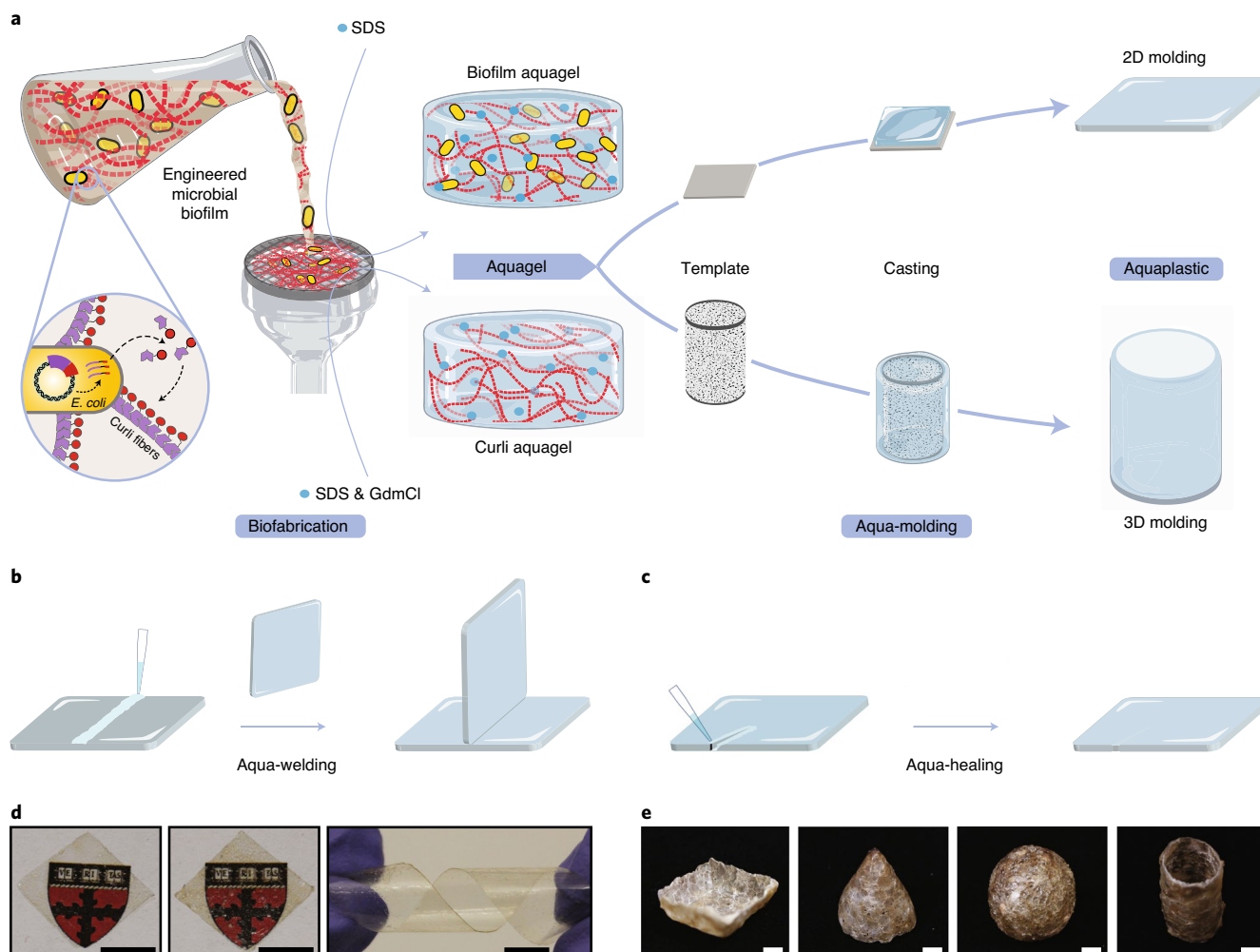
Fig. 1 | Fabrication of aquaplastic directly from engineered microbial biofilms. a–c, Schematics of aquaplastic fabrication from genetically engineered bacteria programmed to produce a functional curli fiber-based aquagel that can be molded into two- (2D) and three-dimensional (3D) architectures (**a**), and aqua-welding (**b**) and aqua-healing (**c**) of aquaplastics. SDS, sodium dodecyl sulfate; GdmCl, guanidinium chloride. **d**, Images of biofilm aquaplastic (left), curli aquaplastic (middle) and the flexibility of biofilm aquaplastic (right). Scale bars, 0.5 cm. **e**, Images of 3D-molded aquaplastic: bowl, cone, sphere and cylinder. Scale bars, 1 cm.

serve as a platform for the biological fabrication of numerous functional materials[2,7,8,11,17]. In one specific example, fusions of the curli fiber monomer, CsgA, to a human cytokine, trefoil factor 2 (TFF2), enabled us to harvest hydrogels simply by filtering bacterial cultures, using sodium dodecyl sulfate (SDS) as a gelator (Supplementary Table 1 and Supplementary Fig. 1)[18,19]. In this work, we denote these hydrogels as either biofilm aquagels, which contain viable bacterial cells, or curli aquagels, which are inert gels from which the cells have been removed. Here, we show that both types of gel can be cast onto surfaces or molds to create plastic films, which we call biofilm aquaplastic and curli aquaplastic, respectively.

Unlike traditional thermoplastics and thermoset plastics, which are melted at high temperatures to form semi-solids that are then molded into desired shapes, aquaplastics are made by casting the aquagels on a template with the desired shape and drying them under ambient conditions to mold their form. When the biofilm/curli aquagels are cast on a flexible or soft flat surface, they form plastic films that can be easily peeled off to form free-standing structures (Fig. 1d and Supplementary Fig. 1). For the biofilm aquaplastics, these films were flexible enough to be twisted repeatedly into heli-

cal shapes without wrinkling or cracking (Supplementary Fig. 2). Because of the remarkable robustness of the constituent curli fibers, the biofilm aquaplastics can also be molded into three-dimensional (3D) architectures, such as cones, bowls, tubes and hollow spheres, by casting them on a sacrificial polystyrene foam mold, followed by selective dissolution of the mold (Fig. 1e and Supplementary Fig. 3).

Physical and chemical properties of aquaplastic. Thermogravimetric analysis (TGA) showed that both the biofilm aquaplastic and curli aquaplastic start to degrade above 200 °C (Fig. 2a and Supplementary Fig. 4). Differential scanning calorimetric (DSC) analysis of the aquaplastics revealed glass transitions for biofilm aquaplastic and curli aquaplastic at 150 °C and 145 °C, respectively, during the cooling cycles (Fig. 2b and Supplementary Fig. 5). Wide-angle X-ray scattering analysis (WAXS) on both biofilm aquaplastic and curli aquaplastic revealed the characteristic signatures of a cross-β secondary structure of CsgA with d-spacing (interplanar spacing) values of 0.98 nm and 0.46 nm (Fig. 2c and Supplementary Fig. 6), corresponding to the inter- and intra-β-sheet distances, respectively, and indicating that the curli
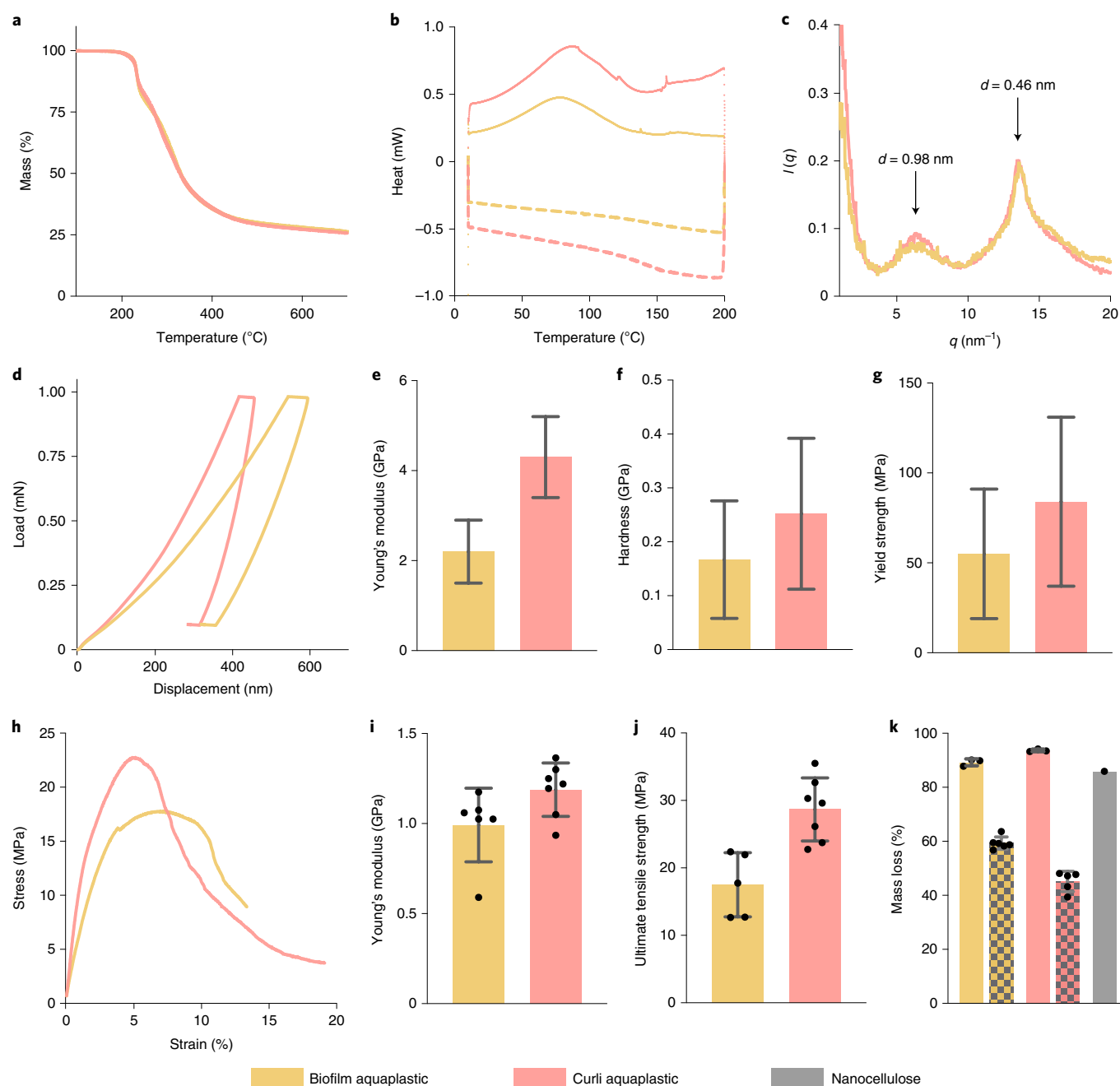
Fig. 2 | Physical and chemical properties of aquaplastics. a–c, TGA thermograms (**a**), DSC thermograms (**b**; heating cycle, solid lines; cooling cycle, dashed lines) and WAXS intensity profiles (**c**) of biofilm aquaplastic and curli aquaplastic. **d–g**, Mechanical properties of biofilm aquaplastic and curli aquaplastic obtained by nanoindentation tests: load–displacement curves under a maximum indentation load of 1 mN in a single indentation cycle (**d**), Young's modulus (**e**), hardness (**f**) and yield strength (**g**). $n = 128$ for biofilm aquaplastic and $n = 82$ for curli aquaplastic. **h–j**, Mechanical properties of biofilm aquaplastic and curli aquaplastic obtained by tensile tests: stress–strain curves (**h**), Young's modulus (**i**) and ultimate tensile strength (**j**). **k**, Biodegradation analysis of biofilm aquaplastic and curli aquaplastic, compared to nanocellulose, based on mass loss after exposure to a wastewater-derived microbial consortium. The patterned bars correspond to mass loss of biofilm aquaplastic and curli aquaplastic due to dissolution of water-soluble sub-components in water. The bar graphs represent mean values, and the error bars are standard deviation.

amyloid structure is maintained through the aquaplastic processing steps[20]. The mechanical properties of the aquaplastics were first investigated by nanoindentation, which showed Young's modulus values (E) of 2.2 ± 0.7 GPa (biofilm aquaplastic) and 4.3 ± 0.9 GPa (curli aquaplastic), respectively (Fig. 2d–g)[21]. The corresponding hardness (H) values at maximum load were found to be 167 ± 109 MPa and 252 ± 140 MPa, while the yield strength (σ_y) values (estimated using the relation $\sigma_y = H/3$) were 55 ± 36 MPa

and 84 ± 47 MPa, respectively[22]. Tensile tests performed on aquaplastic films clearly showed the plastic deformation of the material (Fig. 2h). The biofilm aquaplastic exhibited $E = 1 \pm 0.2$ GPa (Fig. 2i), an ultimate tensile strength (σ) of 18 ± 5 MPa (Fig. 2j) and tensile toughness (U_T) of 102 ± 57 MJ m^{-3} (Supplementary Fig. 7). The curli aquaplastic was found to have E, σ and U_T values of 1.2 ± 0.2 GPa, 29 ± 5 MPa and 261 ± 77 MJ m^{-3}, respectively. Supplementary Table 2 compares the mechanical properties of biofilm aquaplastic
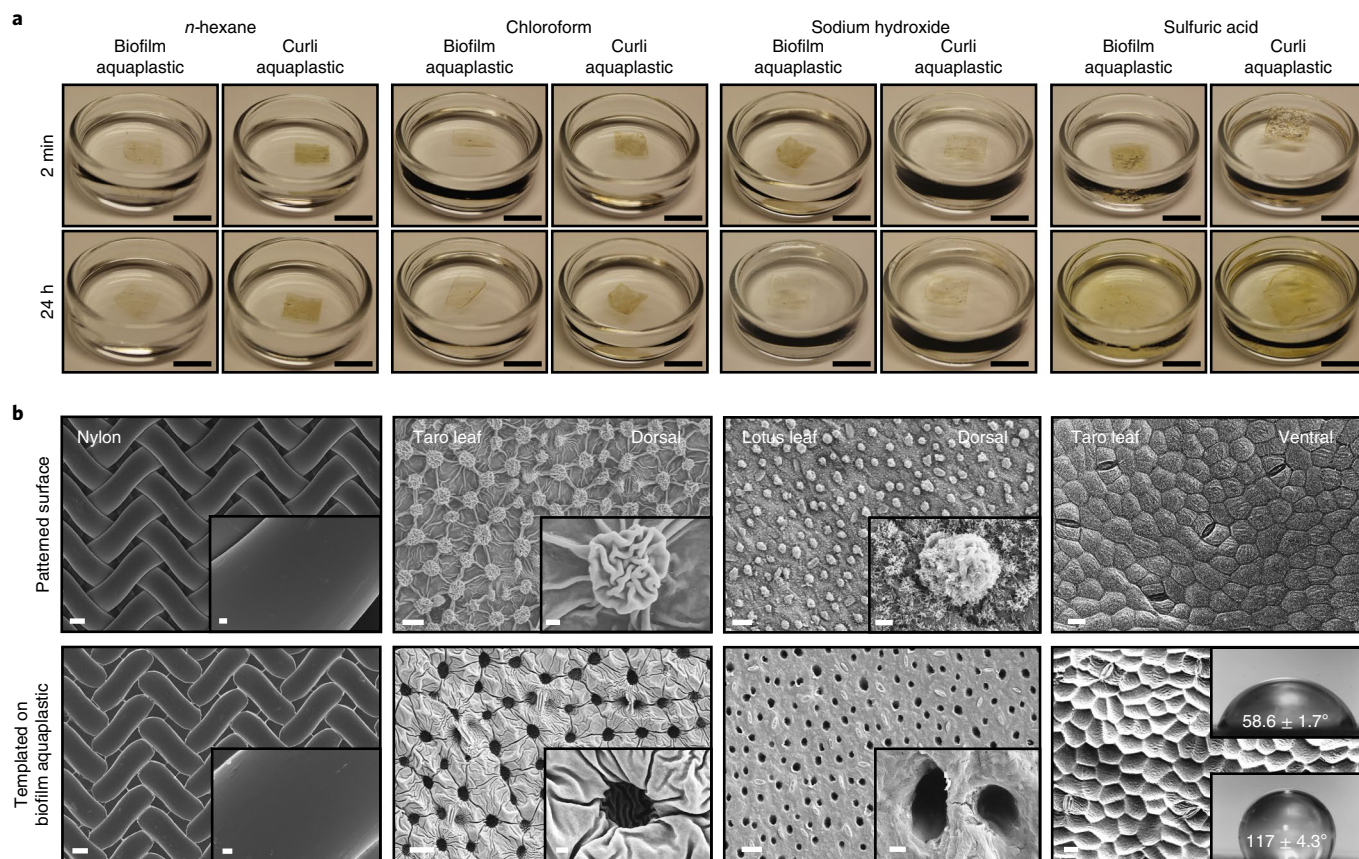
Fig. 3 | Chemically resistant aquaplastic and its templated surface structure properties. a, Images showing the stability of a 1-cm² sample of aquaplastic in organic solvents (*n*-hexane, chloroform), strong acid (98% sulfuric acid) and strong base (18 M sodium hydroxide) after 2 min or 24 h of exposure. Scale bars, 1 cm. **b**, Field-emission scanning electron microscopy (FESEM) images showing the patterns transferred (bottom row) on biofilm aquaplastic by templating biofilm aquagel on various surfaces (top row) by ambient drying. Scale bars, 20 μm. Insets in the first three columns show higher magnifications of surface features. Scale bars, 2 μm. Insets in the rightmost column are water contact angles for non-templated (top) and templated aquaplastic surfaces (bottom), showing increased hydrophobicity.

and curli aquaplastic with those of petrochemical plastics and other bioplastics.

The biodegradability of the aquaplastic was investigated under aerobic conditions by incubating them for 45 days in the presence of a mixed culture of microorganisms obtained from the primary effluent of a wastewater treatment plant[23]. Microorganisms in the mixed culture media metabolize samples into biogas and water-soluble species (that is, ions or simple protein/sugars), resulting in mass loss for each sample. The aquaplastics were compared to nanocellulose, which is known to undergo rapid and complete biodegradation. Both biofilm aquaplastic and curli aquaplastic were found to lose 94% and 89% of their initial masses, respectively, over the course of 45 days, while the positive control—nanocellulose—lost 85% mass over the same time span (Fig. 2k). As negative controls, biofilm aquaplastic and curli aquaplastic were incubated in milliQ water without the degrading microorganisms, leading to nearly 59% and 45% mass loss, respectively, that could be attributed to dissolution of SDS and other water-soluble cellular components. Indeed, square sheets of biofilm aquaplastic and curli aquaplastic, when immersed in water, swell to 324% and 225% in terms of their lateral dimensions, respectively (Supplementary Fig. 8). After several water washes, both aquaplastic films shrink back to their original dimensions, leaving behind transparent and water-insoluble films of curli nanofibers. Therefore, the mass losses observed in the biodegradation experiments (Fig. 2k) reflect a composite of dissolution and biodegradation of the remaining protein-enriched material.

Although the aquaplastics are biodegradable, their constituent curli fibers are also known to be resistant to disassembly in the presence of solvents, harsh pH values and detergents[24]. We found that both aquaplastics were stable in non-polar solvents like *n*-hexane, even after 24 h of incubation (Fig. 3a and Supplementary Figs. 9 and 10). Aquaplastics were also stable in chloroform, which is known to dissolve coatings, rubber and many plastics such as polystyrene and polyvinyl chloride (Fig. 3a and Supplementary Fig. 9). The weight of aquaplastics did not change appreciably after incubation in the organic solvents (Supplementary Fig. 9). Surprisingly, both aquaplastics remained intact and unchanged after 24 h in 18 M sodium hydroxide (Fig. 3a and Supplementary Fig. 11). On the other hand, upon incubation in concentrated sulfuric acid (98%), both aquaplastics formed gelatinous films with double the original film dimensions within a few minutes (Fig. 3a and Supplementary Fig. 11). The biofilm aquaplastic disintegrated into smaller fragments, while the curli aquaplastic lost ~45% of its mass in concentrated sulfuric acid (Supplementary Fig. 9). Similar exposures to concentrated nitric acid (70%) and concentrated hydrochloric acid (35%) led to a slight yellow coloration and degradation of both aquaplastics within a couple of hours (Supplementary Figs. 11 and 12). Thus, it might be that the Na⁺ and sulfate groups of SDS, in association with the curli fibers and other components of the aquaplastic, provide a protective barrier in acidic and basic conditions. Aquaplastic films incubated in sodium hydroxide had salts precipitated on their surface, which we could not remove
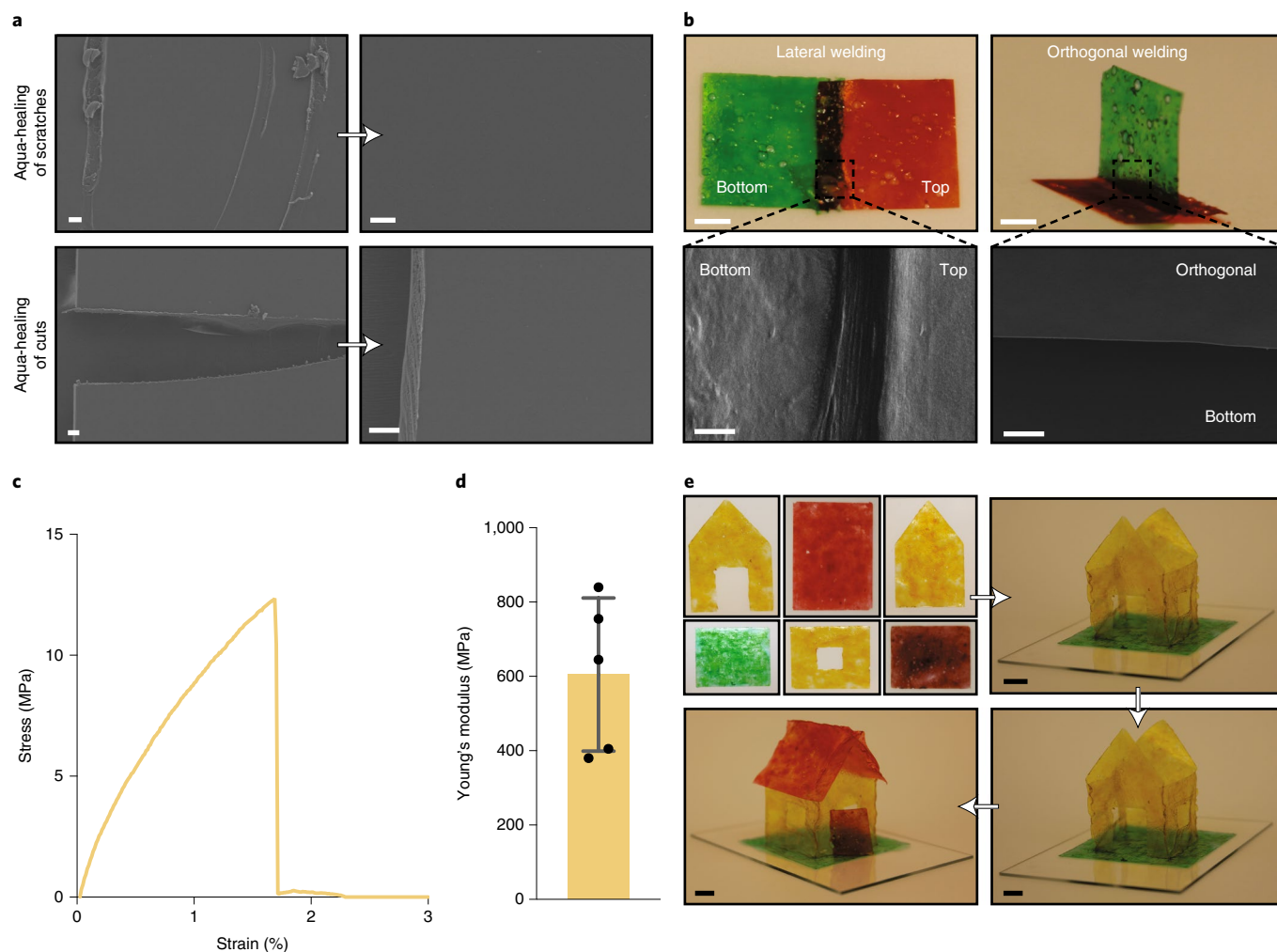
Fig. 4 | Aqua-healing and aqua-welding of aquaplastic. a, Scratches and cuts of biofilm aquaplastic were aqua-healed by adding water at the site of abrasion. Scale bars, 20 μm. **b**, Aqua-welding of two biofilm aquaplastic panels in parallel and perpendicular orientations. Scale bars, 5 mm (optical images) and 20 μm (FESEM images). **c**, Stress–strain curve of aqua-welded biofilm aquaplastic. **d**, Young's modulus obtained by tensile tests of aqua-welded biofilm aquaplastic ($n = 5$). The bar graph shows mean values. Error bars represent standard deviation. **e**, A 3D architecture, an aquaplastic house, constructed by aqua-welding 2D panels. Scale bars, 1 cm.

completely, and accurate weight values could not be determined for mass loss analysis.

Templated and coatable aquaplastic. The chemical resistance of aquaplastics and the known adhesive properties of curli fibers further inspired us to fabricate protective coatings, which are currently made with non-biodegradable plastics[9]. Unlike traditional plastic powder-based coating strategies[25], aquaplastic coatings were formed by casting aquagels onto various surfaces followed by air-drying under ambient conditions. Aquaplastics could be applied easily to create strongly adhered coatings on convoluted surfaces, like leather or plywood, or on flat surfaces, such as mobile phone touch screens, aluminum automobile exterior body parts and copper wire (Extended Data Fig. 1). The results not only demonstrate the versatility of aquaplastics to conform to different shapes (1D wires and 2D surfaces), but also their ability to firmly adhere to materials with a range of roughnesses and compositions (for example, biomaterials, electronics and metals).

Another feature of aquaplastic fabrication is the ability to template patterns onto its surface during the drying process. For aquaplastics of either type, drying of the gel precursors on nylon

meshes composed of 30- to 35-μm-wide fibers led to transfer of the mesh pattern onto the dried film with high fidelity (Fig. 3b and Supplementary Fig. 13). More irregular patterns could also be templated onto aquaplastics this way. Leaves of *Colocasia esculenta* (taro) are known to be hydrophobic on their dorsal side due in part to their surface nanotopography. After casting aquaplastics on the leaf and peeling them off to form self-standing films, we observed pockets formed on the film surface by the 10- to 15-μm mushroom-like structures on the leaf surface (Fig. 3b), along with other features down to ~1 μm. We tested the size resolution limits of this templating by casting aquaplastics on the dorsal surface of a *Nelumbo nucifera* (lotus) leaf. In addition to the characteristic papillae structures (pillars with diameters of 5–10 μm) from the leaf surface, the aquaplastics successfully captured leaf surface features as small as ~30 nm, originating from waxy crystalline aggregates (Fig. 3b and Supplementary Figs. 13 and 14). This templating capability could also be leveraged to alter surface wettability, with aquaplastics cast on the ventral surface of the hydrophobic taro leaf being imparted with hydrophobic characteristics (contact angle of $117° ± 4.3°$) that result from the leaf nanotopography, compared to non-templated surfaces (contact angle of $58.6° ± 1.7°$; Fig. 3b)[26].

Water-processable aquaplastic. Although the tendency of aquaplastics to rehydrate upon exposure to water hinders their direct comparison to petrochemical plastics for certain applications[27,28], it does lead to unusual and possibly beneficial material performance characteristics. We exploited the water-responsiveness of the aquaplastics to demonstrate their ability to self-heal. Scratches made on the surface of a biofilm aquaplastic could be removed completely by spraying a few microliters of water onto the scratch and allowing it to air-dry for 2 min (Fig. 4a). Full-thickness cuts in the biofilm aquaplastic could be healed in a similar manner. Curli aquaplastic could also heal but slightly less efficiently, showing 'scars' after the aqua-healing process when analyzed by field-emission scanning electron microscopy (FESEM; Supplementary Fig. 15). Using a similar protocol, independently fabricated aquaplastic films could be 'aqua-welded' together using only water to trigger their adhesive properties. Rectangular aquaplastic films could be attached to one another in perpendicular and parallel (overlapping) orientations just by spraying water at the interface and allowing for 2 min of drying (Fig. 4b and Supplementary Fig. 16). Tensile tests on laterally aqua-welded films exhibited $E = 605 \pm 206$ MPa, indicating that aquaplastic can be welded effectively with water (Fig. 4c,d). This strategy could be leveraged to create self-standing 3D structures, such as a miniature house with a footprint of 4 cm × 4 cm, composed of 10 aqua-welded panels (Fig. 4e). Notably, the aqua-welded house was strong enough to support its own weight for at least 18 months after its original construction.

Discussion

None of the properties described for the aquaplastics above applies to the wild-type CsgA protein, despite its ability to self-assemble into fibrous structures. We found that both the fused TFF2 (or other protein) domains and the presence of SDS in the washes was necessary to arrive at a hydrogel, which, when dried, exhibited moldable properties. Our preliminary data support the conclusion that both factors contribute to the formation of a hydrated network of curli fiber polymers that adopts a plastic state upon drying, whereas in the absence of either feature (CsgA fusion or SDS-induced gelation), the protocol leads to brittle films that crack upon drying (Supplementary Fig. 17). These observations are also consistent with SDS's known role as a gelator, although this is the first report of its role as a plasticizer.

In general, solvent-cast biopolymer films often form amorphous (soft) or crystalline (rigid) structures upon drying, hindering their utility as plastics that can hold a 3D shape[29–33]. However, several proteins (for example, silk and suckerein), polysaccharides (for example, chitin and starch) and their blends have been shown to form bioplastics[34–36]. Aquaplastic technology provides an opportunity to fabricate 3D structures without having to carry out rigorous purification or material processing. It combines the features of moldability into arbitrary 3D shapes, complete water processability, ambient fabrication, microbial production and genetic programmability. These properties result in a biomaterial fabrication platform with considerably more versatility in material properties than other microbially derived bioplastics, such as polylactides and polyhydroxyalkanoates. Ongoing work will focus on increasing the yield and production scale of the curli fiber-based bioplastics (currently at 100 mg of aquaplastic per liter of bacterial culture) and exploring the use of engineered curli fibers with various fused domains in conjunction with other materials to form composite materials with an even wider range of properties relevant for plastics. By employing an optimized chassis with advanced pathways in bioreactors, the production yields can be increased further by one to two orders of magnitude. These efforts, in addition to advances in biomanufacturing technology and synthetic biology, will provide opportunities for the production of biodegradable plastics from sustainably derived molecular components and energy sources.

Online content

Any methods, additional references, Nature Research reporting summaries, source data, extended data, supplementary information, acknowledgements, peer review information; details of author contributions and competing interests; and statements of data and code availability are available at https://doi.org/10.1038/s41589-021-00773-y.

References

1. Khalil, A. S. & Collins, J. J. Synthetic biology: applications come of age. *Nat. Rev. Genet.* **11**, 367–379 (2010).
2. Nguyen, P. Q., Courchesne, N. D., Duraj-Thatte, A., Praveschotinunt, P. & Joshi, N. S. Engineered living materials: prospects and challenges for using biological systems to direct the assembly of smart materials. *Adv. Mater.* **30**, e1704847 (2018).
3. Chen, A. Y., Zhong, C. & Lu, T. K. Engineering living functional materials. *ACS Synth. Biol.* **4**, 8–11 (2015).
4. Gilbert, C. & Ellis, T. Biological engineered living materials: growing functional materials with genetically programmable properties. *ACS Synth. Biol.* **8**, 1–15 (2019).
5. Duraj-Thatte, A. M. et al. Genetically programmable self-regenerating bacterial hydrogels. *Adv. Mater.* **31**, e1901826 (2019).
6. Botyanszki, Z., Tay, P. K., Nguyen, P. Q., Nussbaumer, M. G. & Joshi, N. S. Engineered catalytic biofilms: site-specific enzyme immobilization onto *E. coli* curli nanofibers. *Biotechnol. Bioeng.* **112**, 2016–2024 (2015).
7. Nguyen, P. Q., Botyanszki, Z., Tay, P. K. & Joshi, N. S. Programmable biofilm-based materials from engineered curli nanofibres. *Nat. Commun.* **5**, 4945 (2014).
8. Chen, A. Y. et al. Synthesis and patterning of tunable multiscale materials with engineered cells. *Nat. Mater.* **13**, 515–523 (2014).
9. Zhong, C. et al. Strong underwater adhesives made by self-assembling multi-protein nanofibres. *Nat. Nanotechnol.* **9**, 858–866 (2014).
10. Gonzalez, L. M., Mukhitov, N. & Voigt, C. A. Resilient living materials built by printing bacterial spores. *Nat. Chem. Biol.* **16**, 126–133 (2020).
11. Tay, P. K. R., Manjula-Basavanna, A. & Joshi, N. S. Repurposing bacterial extracellular matrix for selective and differential abstraction of rare earth elements. *Green Chem.* **20**, 3512–3520 (2018).
12. Liu, X. et al. Stretchable living materials and devices with hydrogel–elastomer hybrids hosting programmed cells. *Proc. Natl Acad. Sci. USA* **114**, 2200–2205 (2017).
13. Geyer, R., Jambeck, J. R. & Law, K. L. Production, use and fate of all plastics ever made. *Sci. Adv.* **3**, e1700782 (2017).
14. Chiellini, E., Corti, A., D'Antone, S. & Solaro, R. Biodegradation of poly (vinyl alcohol) based materials. *Prog. Polym. Sci.* **28**, 963–1014 (2003).
15. Flemming, H. C. & Wingender, J. The biofilm matrix. *Nat. Rev. Microbiol.* **8**, 623–633 (2010).
16. Barnhart, M. M. & Chapman, M. R. Curli biogenesis and function. *Annu. Rev. Microbiol.* **60**, 131–147 (2006).
17. Nussbaumer, M. G. et al. Bootstrapped biocatalysis: biofilm-derived materials as reversibly functionalizable multienzyme surfaces. *ChemCatChem* **9**, 4328–4333 (2017).
18. Duraj-Thatte, A. M., Praveschotinunt, P., Nash, T. R., Ward, F. R. & Joshi, N. S. Modulating bacterial and gut mucosal interactions with engineered biofilm matrix proteins. *Sci. Rep.* **8**, 3475 (2018).
19. Wu, X. et al. Sodium dodecyl sulfate-induced rapid gelation of silk fibroin. *Acta Biomater.* **8**, 2185–2192 (2012).
20. Wei, G. et al. Self-assembling peptide and protein amyloids: from structure to tailored function in nanotechnology. *Chem. Soc. Rev.* **46**, 4661–4708 (2017).
21. Adamcik, J. et al. Measurement of intrinsic properties of amyloid fibrils by the peak force QNM method. *Nanoscale* **4**, 4426–4429 (2012).
22. Avinash, M. B., Raut, D., Mishra, M. K., Ramamurty, U. & Govindaraju, T. Bioinspired reductionistic peptide engineering for exceptional mechanical properties. *Sci. Rep.* **5**, 16070 (2015).
23. Phan, D. C., Goodwin, D. G. Jr, Frank, B. P., Bouwer, E. J. & Fairbrother, D. H. Biodegradability of carbon nanotube/polymer nanocomposites under aerobic mixed culture conditions. *Sci. Total Environ.* **639**, 804–814 (2018).
24. Knowles, T. P. & Mezzenga, R. Amyloid fibrils as building blocks for natural and artificial functional materials. *Adv. Mater.* **28**, 6546–6561 (2016).
25. Du, Z. et al. The review of powder coatings. *Chem. Mater. Sci.* **4**, 54–59 (2016).
26. Avinash, M. B., Verheggen, E., Schmuck, C. & Govindaraju, T. Self-cleaning functional molecular materials. *Angew. Chem. Int. Ed.* **51**, 10324–10328 (2012).

27. Albertsson, A. C. & Hakkarainen, M. Designed to degrade. *Science* **358**, 872–873 (2017).
28. Abdullah, Z. W., Dong, Y., Davies, I. J. & Barbhuiya, S. PVA, PVA blends, and their nanocomposites for biodegradable packaging application. *Polym. Plast. Technol. Eng.* **56**, 1307–1344 (2017).
29. Amsden, J. J. et al. Rapid nanoimprinting of silk fibroin films for biophotonic applications. *Adv. Mater.* **22**, 1746–1749 (2010).
30. Kim, D. H. et al. Dissolvable films of silk fibroin for ultrathin conformal bio-integrated electronics. *Nat. Mater.* **9**, 511–517 (2010).
31. Perry, H., Gopinath, A., Kaplan, D. L., Dal Negro, L. & Omenetto, F. Nano- and micropatterning of optically transparent, mechanically robust, biocompatible silk fibroin films. *Adv. Mater.* **20**, 3070–3072 (2008).
32. Brenckle, M. et al. Methods and applications of multilayer silk fibroin laminates based on spatially controlled welding in protein films. *Adv. Funct. Mater.* **26**, 44–50 (2015).
33. Moreau, D., Chauvet, C., Etienne, F., Rannou, F. P. & Corte, L. Hydrogel films and coatings by swelling-induced gelation. *Proc. Natl Acad. Sci. USA* **113**, 13295–13300 (2016).
34. Fernandez, J. G. & Ingber, D. E. Manufacturing of large-scale functional objects using biodegradable chitosan bioplastic. *Macromol. Mater. Eng.* **299**, 932–938 (2014).
35. Guo, C. et al. Thermoplastic moulding of regenerated silk. *Nat. Mater.* **19**, 102–108 (2020).
36. Latza, V. et al. Multi-scale thermal stability of a hard thermoplastic protein-based material. *Nat. Commun.* **6**, 8313 (2015).

Methods

Cell strains and plasmids. TFF2 was fused to the C terminus of CsgA with an intervening 36-amino-acid flexible linker. The gene encoding the trefoil factor (cTFF2) was synthesized (Integrated DNA Technologies) and cloned by overlap extension into pET21d vector. The plasmids also contained genes encoding for other proteins necessary for curli biosynthesis, including csgC, csgE, csgF and csgG. All experiments used cell strain PQN4, an *E. coli* strain derived from LSR10 (MC4100, ΔcsgA, λ(DE3), Cam^R).

Preparation of biofilm aquagel. Bacterial cultures were incubated at 37 °C for 48 h to express engineered curli fibers, which were concentrated using vacuum filtration through a 47-mm-diameter polycarbonate membrane with 11-μm pores (EMD Millipore). The concentrated biofilm (engineered fibers) was washed with 25 ml of sterile deionized (DI) water on the filter membrane. Next, the biofilm was incubated with 5 ml of gelator/plasticizer comprising 5% (mass/vol) SDS in water for 5 min, followed by vacuum filtration of the liquid, which was then washed with 25 ml of DI water. Biofilm aquagel that formed on the filter membrane was collected and stored at 4 °C.

Preparation of curli aquagel. Functional curli fibers were expressed in bacterial cultures for 48 h, then treated with guanidinium chloride (GdmCl) to a final concentration of 0.8 M and kept at 4 °C for 1 h. Treated cultures were concentrated by filtration, as described for the biofilm aquagel. Next, the curli fibers were treated with 5 ml of 8 M GdmCl for 5 min, followed by vacuum filtration of the liquid with 25 ml of sterile DI water wash to remove bacteria, cellular proteins and other components. The remaining biomass was treated with 5 ml of an aqueous solution (2 μM MgCl$_2$) of nuclease (Benzonase, Sigma-Aldrich, 1.5 U ml^{-1}) for 10 min to remove DNA/RNA bound to the curli fibers. Finally, the curli fibers were incubated with 5 ml of gelator/plasticizer, 5% (mass/vol) SDS in water for 5 min, followed by vacuum filtration of the liquid and a wash with 25 ml of DI water. The curli aquagel was collected and stored at 4 °C.

Fabrication of aquaplastic. For fabrication of 2D aquaplastic sheets, aquagel (biofilm aquagel/curli aquagel) was cast on a flat flexible substrate (plastic wrap, aluminum foil), which, upon overnight drying under ambient conditions, formed aquaplastic (biofilm aquaplastic/curli aquaplastic). Completely dried aquaplastic was carefully peeled off from the surface and stored under ambient conditions.

For fabrication of 3D aquaplastic architectures, various shapes of polystyrene molds (cone, bowl, cylinder and sphere) were cast with biofilm aquagels/curli aquagels and left to dry overnight under ambient conditions. The polystyrene molds were selectively removed by dissolving in chloroform to obtain 3D aquaplastic.

Thermal gravimetric analysis and differential scanning calorimetry. TGA experiments were performed using a Mettler Toledo TGA/DSC 3+ STARe System. Samples (2.6–4.4 mg dry weight) were run at 4 °C min^{-1} under N$_2$ purging at 50 ml min^{-1} in alumina crucibles. DSC measurements were carried out using a Mettler Toledo DSC 1 STARe System. Measurements were run under N$_2$ purging at 30 ml min^{-1} and at 4 °C min^{-1} with 1.8–4.9 mg of sample. Each measurement consisted of a heat–cool–heat cycle in the range of 10–200 °C and was performed in perforated aluminum crucibles. Three experiments were performed for each sample condition and a representative curve is reported.

Wide-angle X-ray scattering. WAXS experiments were performed using a Rigaku MicroMax-002+ equipped with a microfocused beam (40 W, 45 kV, 0.88 mA) with $\lambda_{CuK\alpha} = 0.15418$ nm radiation collimated by three pinhole collimators (0.4, 0.3 and 0.8 mm) to obtain direct information on the scattering patterns. The WAXS intensity was collected by a 2D Fujifilm BAS-MS 2025 imaging plate system (15.2 × 15.2 cm^2, resolution of 50 μm). An effective scattering vector range of 1 nm^{-1} < q < 25 nm^{-1} was obtained, where q is the scattering wavevector defined as $q = 4\pi \sin\theta/\lambda_{CuK\alpha}$ with a scattering angle of 2θ. Three experiments were performed for each sample condition and a representative curve is reported.

Nanoindentation. Biofilm aquagels and curli aquagels were cast on glass cover slips to obtain a topographical thickness of ~50–100 μm. Nanoindentation studies were performed on the samples using an Agilent Technologies G200 nanoindenter. The machine continuously monitored the load (P) and the depth of the penetration (h) of the indenter with resolutions of 1 nN and 0.2 nm, respectively. A Berkovich diamond tip indenter with tip radius of ~100 nm was used for the indentation. A peak load (P_{max}) of 1 mN with loading and unloading rates of 0.2 mN s^{-1} and a hold time (at P_{max}) of 5 s was employed. A minimum of 80 indentations were performed in each case and the average is reported. The P–h curves were analyzed using the Oliver–Pharr method to extract the elastic modulus (E) and the hardness (H) of the samples. The yield strength (σ_y) was estimated using the relation $\sigma_y = H/3$. n = 128 for the biofilm aquaplastic and n = 82 for the curli aquaplastic.

Tensile tests. Tensile measurements were made using a DHR-3 rheometer (TA Instruments), configured with tensile grips. Testing was performed under ambient laboratory conditions. Film specimens were clamped to an initial gauge length of 6 mm. A constant linear deformation of 1 μm s^{-1} was applied (1% strain per minute). The surfaces of the grips were modified with tape at the contact area, to avoid damage to the film specimens during loading. Biofilm aquaplastic and curli aquaplastic films of 3 cm × 1 cm were utilized for tensile tests. For aqua-welding, two biofilm aquaplastic films of 1.5 cm × 1 cm were used and 0.5 cm × 1 cm of the contact area was aqua-welded with water. A minimum of five tests for biofilm aquaplastic and curli aquaplastic were obtained, and the average is reported.

Biodegradation assay. Aerobic biodegradability was determined by measuring the mass loss after exposure to an aerobic mixed culture of microorganisms obtained from the primary effluent of a wastewater treatment plant (Back River Wastewater Treatment Plant). Bacterial medium was made in MilliQ water, and consisted of 10% vol/vol primary effluent, 200 mg l^{-1} sodium acetate trihydrate as a carbon source, and 10% vol/vol of salt stock (7.18 mM K$_2$HPO$_4$, 2.79 mM KH$_2$PO$_4$, 0.757 mM (NH$_4$)$_2$SO$_4$, 0.0406 mM MgSO$_4$.7H$_2$O) as well as trace elements necessary for bacterial growth. Samples were run alongside a nanocellulose positive control, which is known to readily biodegrade in mixed cultures of microorganisms[37]. Approximately 50 mg of each sample was added to 36 ml of blank medium (that is, no cells added yet) in a 50-ml conical vial. n = 3 for the biofilm aquaplastic and curli aquaplastic. Samples were pelletized via centrifuge (4,300 r.p.m., 5 min) to minimize dispersion in the supernatant, and then 4 ml of primary effluent bacteria was introduced to each vial. Samples were shaken (for aeration) at 125 r.p.m. and 28 °C to encourage aerobic bacterial growth. After 45 days of exposure, bacterial supernatant was carefully removed via pipette to avoid disturbing the pellet in the bottom of the vials. This was crucial to avoid the pelletization of biomass and natural organic matter (NOM) into the residual bioplastic samples after biodegradation. At this point, the large majority of NOM and biomass from the vial was removed, allowing for washing of the pellet with 3 × 30 ml of milliQ water, re-centrifuging between each wash without adding artificial mass to the pellet. After washing, the pellets were recovered and dried before massing. Samples were dried first on a hot plate, and then in a vacuum oven. Biodegradation was reported as the percentage of mass lost after 45 days of biodegradation compared to the initial sample mass. Freeze-dried cellulose nanofibrils (CNFs) derived from wood pulp were purchased from the University of Maine Process Development Center. The CNFs were milled to a powder before biodegradation with a FlackTek speed mixer (DAC 150) using 2-mm yttrium-stabilized zirconium milling beads.

Field-emission scanning electron microscopy. FESEM samples were prepared by sputtering a 10- to 20-nm layer of Pt/Pd/Au. Images were acquired using a Zeiss Ultra55/Supra55VP FESEM equipped with a field-emission gun operating at 5–10 kV.

Chemical resistance of aquaplastic. Biofilm aquaplastic and curli aquaplastic (1 cm^2) were fully immersed in the organic solvent (n-hexane, chloroform) and strong acid (98% sulfuric acid) and strong base (18 M sodium hydroxide) for 24 h. The optical images of aquaplastic were taken after 2 min and 24 h of immersion. After 24 h of incubation, the aquaplastic immersed in n-hexane, chloroform, 18 M sodium hydroxide and 98% sulfuric acid was removed and air-dried for 24 h. The weight of aquaplastic before and after the treatment was noted. After the 24 h of incubation, the biofilm aquaplastic disintegrated into smaller fragments in 98% sulfuric acid, while both biofilm aquaplastic and curli aquaplastic had salts precipitated on their surfaces in 18 M sodium hydroxide, which we could not remove completely, and the accurate weight of the aquaplastic films could not be determined. n = 3 for biofilm aquaplastic and curli aquaplastic.

Coating of aquaplastic. Curli aquagel was cast on various surfaces (cow leather, plywood, mobile phone touch screen, automobile exterior aluminum body part and copper wire), which, upon drying under ambient conditions, resulted in aquaplastic-coated surfaces. All surfaces in their coated and uncoated states were imaged by FESEM. n ≥ 3 for biofilm aquaplastic and curli aquaplastic.

Templating aquaplastic. Biofilm aquagel and curli aquagel were cast on various patterned surfaces: nylon, taro leaf (Colocasia esculenta) and lotus leaf (Nelumbo nucifera). Upon overnight drying under ambient conditions, the aquaplastic was peeled off from the surface and imaged using FESEM. n ≥ 3 for biofilm aquaplastic and curli aquaplastic.

Rehydration of aquaplastic. Biofilm aquaplastic and curli aquaplastic (1 cm^2) were incubated in MilliQ water and, within 2 min, the aquaplastic swelled to its maximum capacity. After 2 min, the excess water was wicked off. The aquaplastic films retained their swollen dimensions if dried after rehydrating. The weight and lateral dimensions of the aquaplastic were recorded before and after rehydration. n = 3 for biofilm aquaplastic and curli aquaplastic.

Aqua-healing. Surface scratches and cuts were made to the biofilm aquaplastic and curli aquaplastic. Water (~10 μl) was added at the place of abrasion and, upon air-drying, the aquaplastic was healed. n ≥ 3 for biofilm aquaplastic and curli aquaplastic.

Aqua-welding. Water was employed as a glue to weld two pieces of biofilm aquaplastic or curli aquaplastic. It was found that 10–20 μl of water line spanning

1 cm was enough to weld two aquaplastics with dimensions of 1 cm². $n \geq 3$ for biofilm aquaplastic and curli aquaplastic.

Water-resistant aquaplastic (aquaplastic washed). Washing both biofilm aquaplastic and curli aquaplastic with excess water removed all water-soluble components, such as SDS, and other cellular components, giving rise to a transparent water-insoluble film. Both biofilm aquaplastic and curli aquaplastic initially swell, but with excessive water washing they ultimately shrank to their original lateral dimensions. The water-washed biofilm aquaplastic and curli aquaplastic samples exhibit resistance to water and do not wet. $n \geq 5$ for biofilm aquaplastic and curli aquaplastic.

Statistics and reproducibility. All experiments presented in this Article were repeated at least three times ($n \geq 3$) on distinct samples, as clearly specified in the figure legends or the relevant Methods sections. In all cases, data are presented as the mean and standard deviation. GraphPad Prism 8 software was used for plotting and analyzing data. For micrographs and optical images, we present representative images.

Reporting Summary. Further information on research design is available in the Nature Research Reporting Summary linked to this Article.

Data availability
All relevant data supporting the findings of this study and the plasmids and strains used are available within the Article and its Supplementary Information or from the corresponding authors upon request. Source data are provided with this paper.

References
37. Beguin, P. & Aubert, J. P. The biological degradation of cellulose. *FEMS Microbiol. Rev.* **13**, 25–58 (1994).

Author contributions
A.M.D.-T. and A.M.-B. conceived the idea. A.M.D.-T. and A.M.-B. prepared aquagels, fabricated aquaplastics, tested the chemical resistance of the aquaplastic, performed aquaplastic coating, templating and rehydration studies as well as aqua-healing and aqua-welding. A.M.-B. performed FESEM and nanoindentation studies. N.-M.D.C. and G.I.C. performed initial experiments with aquagels and aquaplastic. A.S.-F. carried out WAXS and DSC studies. L.v.H. performed TGA and DSC studies. B.P.F. performed biodegradation studies. S.K.C. performed tensile tests. D.H.F. supervised B.P.F. R.M. supervised A.S.-F. and L.v.H. A.M.D.-T., A.M.-B. and N.S.J. wrote and/or edited the manuscript. All authors discussed and commented on the manuscript.

Competing interests
A.M.D.-T., N.-M.D.C. and N.S.J. are inventors on patent application WO2017201428A8, submitted by Harvard University.

Additional information
Extended data is available for this paper at https://doi.org/10.1038/s41589-021-00773-y.

Supplementary information The online version contains supplementary material available at https://doi.org/10.1038/s41589-021-00773-y.

Correspondence and requests for materials should be addressed to N.S.J.

Reprints and permissions information is available at www.nature.com/reprints.
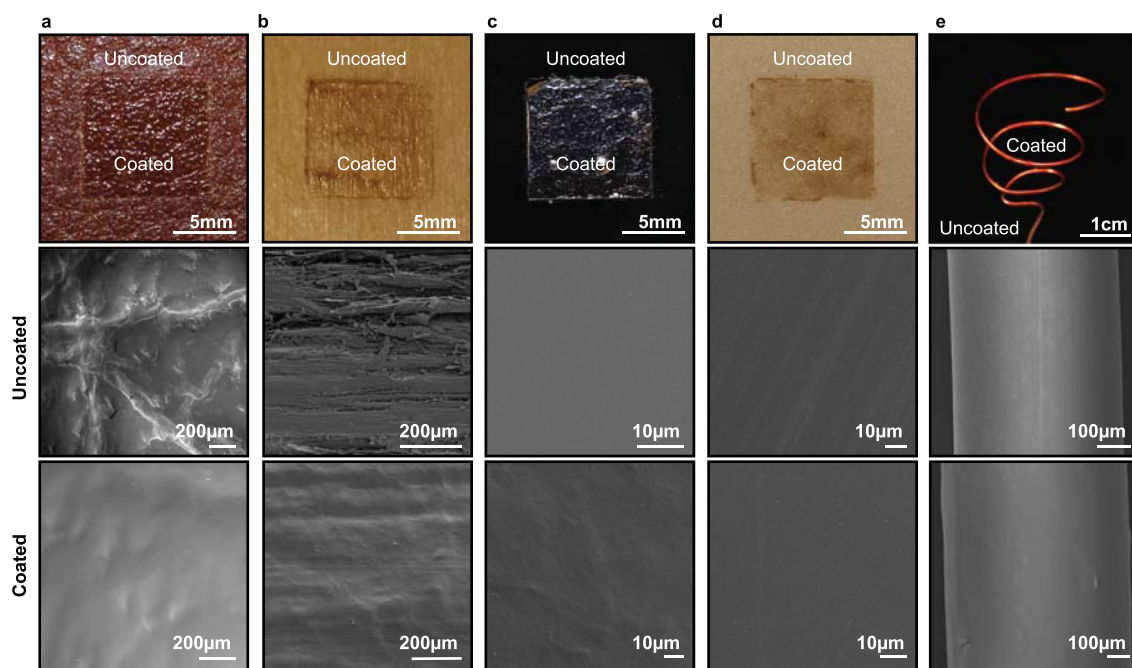
Extended Data Fig. 1 | Coating of curli aquaplastic on various surfaces. Coating of curli aquaplastic on various surfaces. Optical images of **a**. Cow leather, **b**. Plywood **c**. Mobile phone touch screen, **d**. Aluminum automobile exterior body part and **e**. Copper wire coated with curli aquaplastic. FESEM images of coated and uncoated surfaces are shown below.

Corresponding author(s): Neel Joshi

Last updated by author(s): Feb. 05, 2021

Reporting Summary

Nature Research wishes to improve the reproducibility of the work that we publish. This form provides structure for consistency and transparency in reporting. For further information on Nature Research policies, see our Editorial Policies and the Editorial Policy Checklist.

Statistics

For all statistical analyses, confirm that the following items are present in the figure legend, table legend, main text, or Methods section.

n/a	Confirmed	
☐	☒	The exact sample size (*n*) for each experimental group/condition, given as a discrete number and unit of measurement
☐	☒	A statement on whether measurements were taken from distinct samples or whether the same sample was measured repeatedly
☒	☐	The statistical test(s) used AND whether they are one- or two-sided *Only common tests should be described solely by name; describe more complex techniques in the Methods section.*
☒	☐	A description of all covariates tested
☒	☐	A description of any assumptions or corrections, such as tests of normality and adjustment for multiple comparisons
☐	☒	A full description of the statistical parameters including central tendency (e.g. means) or other basic estimates (e.g. regression coefficient) AND variation (e.g. standard deviation) or associated estimates of uncertainty (e.g. confidence intervals)
☒	☐	For null hypothesis testing, the test statistic (e.g. *F*, *t*, *r*) with confidence intervals, effect sizes, degrees of freedom and *P* value noted *Give P values as exact values whenever suitable.*
☒	☐	For Bayesian analysis, information on the choice of priors and Markov chain Monte Carlo settings
☒	☐	For hierarchical and complex designs, identification of the appropriate level for tests and full reporting of outcomes
☒	☐	Estimates of effect sizes (e.g. Cohen's *d*, Pearson's *r*), indicating how they were calculated

Our web collection on statistics for biologists contains articles on many of the points above.

Software and code

Policy information about availability of computer code

Data collection	No software was used for data collection
Data analysis	GraphPad PRISM 8

For manuscripts utilizing custom algorithms or software that are central to the research but not yet described in published literature, software must be made available to editors and reviewers. We strongly encourage code deposition in a community repository (e.g. GitHub). See the Nature Research guidelines for submitting code & software for further information.

Data

Policy information about availability of data

All manuscripts must include a data availability statement. This statement should provide the following information, where applicable:
- Accession codes, unique identifiers, or web links for publicly available datasets
- A list of figures that have associated raw data
- A description of any restrictions on data availability

We do not have any data derived from public databases or that belongs in public databases. We have included a section entitled "Data and Materials Availability" to indicate how people can request access to these from the corresponding author.

Field-specific reporting

Please select the one below that is the best fit for your research. If you are not sure, read the appropriate sections before making your selection.

☒ Life sciences   ☐ Behavioural & social sciences   ☐ Ecological, evolutionary & environmental sciences

For a reference copy of the document with all sections, see nature.com/documents/nr-reporting-summary-flat.pdf

Life sciences study design

All studies must disclose on these points even when the disclosure is negative.

Sample size	Sample sizes were arbitrary because the all the samples are materials. The replicates were done only to show the distribution of values that were obtained. Because we are not making any statistical comparisons between sample cohorts, there is no need for more sophisticated methods for sample size determination.
Data exclusions	No data was excluded
Replication	All experiments were performed in at least triplicate. All attempts at replication were successful, with the bars and error bars in each relevant plot representing the mean and standard deviation of the replicates, respectively.
Randomization	Randomization between sample cohorts was not possible for any experiments because the cohorts are materials with different compositions.
Blinding	TGA, SAXS,, DSC, and tensile testing were all performed in a blinded manner. The originator lab shipped samples with blinded labels to the collaborating lab. Therefore the researchers performing the analyses were unaware of which cohort the samples belonged to.

Reporting for specific materials, systems and methods

We require information from authors about some types of materials, experimental systems and methods used in many studies. Here, indicate whether each material, system or method listed is relevant to your study. If you are not sure if a list item applies to your research, read the appropriate section before selecting a response.

Materials & experimental systems

n/a	Involved in the study
☒	☐ Antibodies
☒	☐ Eukaryotic cell lines
☒	☐ Palaeontology and archaeology
☒	☐ Animals and other organisms
☒	☐ Human research participants
☒	☐ Clinical data
☒	☐ Dual use research of concern

Methods

n/a	Involved in the study
☒	☐ ChIP-seq
☒	☐ Flow cytometry
☒	☐ MRI-based neuroimaging